Journal of Drug Delivery Science and Technology 105 (2025) 106680

Contents lists available at ScienceDirect

Journal of Drug Delivery Science and Technology

journal homepage: www.elsevier.com/locate/jddst

Regional brain distribution of PLGA nanoparticles functionalized with glutathione or phenylalanine dipeptide

Mario Alonso [a], Emilia Barcia [b,c,*], Sofía Negro [b,c,**], Nicola Paccione [d], Mahdieh Rahmani [b], Consuelo Montejo [a], Luis García-García [e], Ana Fernández-Carballido [b,c]

[a] Department of Health and Pharmaceutical Sciences, School of Pharmacy, Universidad San Pablo-CEU, CEU Universities, 28668, Madrid, Spain
[b] Department of Pharmaceutics and Food Technology, School of Pharmacy, Complutense University of Madrid, 28040, Madrid, Spain
[c] Institute of Industrial Pharmacy, Complutense University of Madrid, 28040, Madrid, Spain
[d] NanoBioCel Group, Department of Pharmacy and Food Science, School of Pharmacy, University of the Basque Country, 01006, Vitoria-Gasteiz, Spain
[e] Multidisciplinary Institute, Complutense University of Madrid, 28040, Madrid, Spain

ARTICLE INFO

Keywords:
Nanoparticles
Blood-brain barrier
PLGA
Glutathione
Phenylalanine
Hippocampus

ABSTRACT

Neurodegenerative diseases are chronic disorders affecting millions of people with their prevalence constantly increasing worldwide. The blood-brain barrier plays a key role in the design of successful treatments for these pathologies. Nanotechnology has the potential to improve treatment of CNS disorders and facilitate effective drug transfer. For this, biodegradable poly (lactic-co-glycolic acid) nanoparticles (PLGA NPs) are promising strategies as they can be surface-tailored with functionalized molecules for site-specific brain targeting. In our work PLGA NPs loaded with a fluorescent marker (rhodamine B) and functionalized with glutathione or phenylalanine dipeptide have been developed, characterized and analyzed for their passage across the BBB and distribution in different brain areas of Wistar rats.

Surface functionalization of the NPs with glutathione or phenylalanine (formulations NP-GSH-Rh and NP-PHE2-Rh) favoured their passage across the BBB process in which glutathione transporter and L-type amino acid transporter 1 (LAT-1) may be involved. One hour after their administration both functionalized formulations predominantly reached the hippocampus followed by the cortex and substantia nigra. Average values of intensity of fluorescence reached in the hippocampus showed statistically significant differences when compared to non-functionalized NPs and remained higher in this area 2 h after administration which allows us to highlight the potential importance of the results obtained as the presence of the NPs in the brain 2 h after their administration counteracts the efflux activity of the P-glycoprotein. In addition, none of the nanosystems caused tissue damage in the hippocampus, cortex or substantia nigra.

1. Introduction

Neurodegenerative diseases are chronic disorders affecting millions of people worldwide, with Alzheimer's disease and Parkinson's disease being the two most prevalent. Many of the drugs with possible therapeutic effects on these diseases fail to access the site of action due to their inability to cross the blood-brain barrier (BBB), a selective barrier formed by endothelial cells that only allows the passage of some substances preventing the majority of drugs from reaching the CNS.

ATP-driven drug efflux pumps (ATP-binding cassette (ABC) transporters) also contribute to maintain brain homeostasis by excreting possible neurotoxic substances. Active pharmaceutical ingredients can also be substrates of these efflux proteins and therefore be expelled. Among the efflux proteins present in the BBB, the most extensively described are the P-glycoprotein (P-gp), the multidrug resistance-associated proteins (MRPs) and the breast cancer resistance protein (BCRP). Due to their ability to transport a large variety of compounds, these efflux proteins represent a significant obstacle for drugs to cross the BBB [1].

Transport of essential molecules to the brain such as nutrients (glucose, galactose, etc.), some amino acids, nucleosides, purines, amines or vitamins is mediated by different transporters that are present

* Corresponding author. Department of Pharmaceutics and Food Technology, School of Pharmacy, Complutense University of Madrid, 28040, Madrid, Spain.
** Corresponding author. Department of Pharmaceutics and Food Technology, School of Pharmacy, Complutense University of Madrid, 28040, Madrid, Spain.
E-mail addresses: ebarcia@ucm.es (E. Barcia), soneal@ucm.es (S. Negro).

https://doi.org/10.1016/j.jddst.2025.106680
Received 19 December 2024; Received in revised form 23 January 2025; Accepted 3 February 2025
Available online 4 February 2025

on the luminal and basolateral sides of the endothelial cells. For this, there is a great variety of transport proteins, for instance, brain cerebral type 1 transporter (GLUT-1), large amino acid transporters (LAT), and nucleoside transporters. Their substrates can therefore cross the BBB through carrier-mediated transport being these carriers size- and stereo-selective [2,3].

Drugs unable to freely cross the BBB can be incorporated into nanosystems although not all nanosystems are able to cross it properly, since their passage depends on several factors such as size, charge, surface properties, and administration route, that must be considered when developing a nanocarrier for this purpose. In this regard, the main routes involved in the passage of nanosystems through the BBB require the use of transporters, adsorption-mediated transcytosis and receptors, also including passive diffusion [4,5].

Small nanoparticles (NPs) are able to cross the BBB more easily than larger ones although functionalization or coating their surfaces with suitable molecules may help enhancing the passage of larger nanoparticles through the BBB. For this, active targeting can be explored by means of modifying the surface of NPs using molecules that can be specifically recognized by overexpressed receptors or transporters (transferrin, LDL or integrin αvβ3 receptors, glucose, glutathione or amino acid transporters) thereby causing an increase in the elimination half-life of the drug, due to the binding capacity of the system to the endothelial receptors of the BBB [6]. When using small ligands such as glutathione or maltobionic acid this approach may improve the binding affinity to the target receptors [7]. In fact, sizes of NPs between 170 and 340 nm seem to have less impact on their ability to cross the BBB than the functionalization process [8].

Once functionalized NPs cross the BBB, their distribution within the brain can be affected by physiological factors such as age, the animal model used in the study, as well as the type of ligand used for their functionalization [9,10]. This sectional brain distribution may be important depending on the neurodegenerative disorder to be treated. For instance, in Alzheimer's disease the most affected areas of the brain are the hippocampus and the cortex, whereas in Parkinson's disease is the substantia nigra.

Polymeric nanoparticles also show interesting features including excellent biocompatibility, stability, controlled release of the active ingredient and simple manufacturing [11]. In addition, NPs elaborated with low molecular weight polylactic-co-glycolic acid (PLGA) can be easily functionalized from the carboxyl groups of the polymer.

In our work PLGA NPs loaded with a fluorescent marker (rhodamine B) and functionalized with glutathione or phenylalanine dipeptide have been developed, characterized and analyzed for their passage across the BBB. Also studied is the influence of surface functionalization in their distribution in different areas of the brain of Wistar rats.

2. Materials and methods

2.1. Materials

Rhodamine B (Rh-B), phenylalanine dipeptide (PHE2), glutathione (GSH) and 1-ethyl-3-(3-dimethylaminopropyl)-carbodiimide (EDC) were obtained from Sigma-Aldrich Química, S.A. (Madrid, Spain). The reagents (2-(N-morpholino) ethanesulfonic acid) (MES), N-hidroxysuccinimide (NHS), Ellman's reagent (DTNB, 5,5′-dithiobis-(2-nitrobenzoic acid) and 4′,6-diamidino-2-phenylindole (DAPI) were obtained from Thermo Fisher Scientific (Madrid, Spain). PLGA Resomer® RG 502 (Poly(D,L-lactide-co-glycolide) 50:50, Mw 12,000 Da) was provided by Evonik Industries AG (Essen, Germany). Dichloromethane (DCM), methanol, polyvinyl alcohol (PVA, Mw 30,000–70,000 Da) were provided by Sigma-Aldrich Química, S.A. (Madrid, Spain). All buffers and solutions were prepared with distilled and deionized water (Q-POD® Milli-Q system, Merck Millipore, Madrid, Spain).

2.2. Elaboration of nanoparticles

Three formulations of Rh-B loaded PLGA NPs were prepared by the solvent extraction-evaporation method (Table 1). Briefly, 50 mg of PLGA 502 and 2.5 mg of Rh-B were dissolved in 2 mL of DCM. The resulting solution was added dropwise into 6 mL of a 1.5 % PVA solution. Both phases were sonicated at 80 % amplitude for 10 min in pulses (15 s on, 10 s off). The organic solvent was removed under magnetic stirring for 4 h. The NPs were washed three times with water and centrifuged at 20,150 g for 30 min (Sorvall ST 8R centrifuge, Thermo Fisher Scientific, Waltham, USA). Finally, the NPs were suspended in 1 mL of a 1.5 % sucrose solution (cryoprotectant) and freeze-dried for 24 h (Lyo Quest®, Azbil Telstar® S.A., Madrid, Spain). Thereafter, phenylalanine dipeptide (PHE2) and glutathione (GSH) were linked to this formulation (NP-Rh) to obtain NPs functionalized with either PHE2 (formulation NP-PHE2-Rh) or GSH (formulation NP-GSH-Rh) (Table 1).

2.3. Functionalization of nanoparticles with glutathione

Formulation NP-Rh was functionalized with GSH by binding the peptide onto the surface of the NPs after activating the carboxyl groups of PLGA. Firstly, the NPs were maintained at 4 °C for 24 h in 1 mL of distilled water, following the procedure described by Constantino et al. [12] adapted to our experimental conditions. For this, 55 mg of formulation NP-Rh suspended in 1 mL of distilled water were added to 0.5 mL of a buffered solution of 0.1M (2-(N-morpholino)ethanesulfonic acid) (MES) at pH 4.7. To this solution, 50 mg of N-hydroxysuccinimide (NHS) were added.

Then, 150 mg of 1-ethyl-3(3-dimethylamino-propyl) carbodiimide hydrochloride (EDC) dissolved in 2.5 mL of MES buffer were added. The nanoparticle suspension was kept under magnetic stirring for 1 h and then centrifuged at 20,150 g for 25 min to remove the MES buffer along with any unreacted reagent.

Then, the NPs were suspended in 2.5 mL of phosphate buffer (PBS) (Thermo Fisher Scientific, Madrid, Spain) adjusted to pH 7.4. To this second suspension, 2 mg of GSH dissolved in 2.5 mL of PBS at pH 7.4 were added with the admixture kept under magnetic stirring for 2 h to ensure the reaction. Then, the NPs were centrifuged at 20,150 g for 30 min, the cryoprotectant (1.5 % sucrose) added and the NPs (formulation NP-GSH-Rh) freeze-dried for 24 h. The supernatant PBS was collected and the amount of GSH not bound to the surface of the NPs was quantified. All formulations were prepared in triplicate.

2.4. Quantification of GSH bound to the nanoparticles

Quantification of GSH bound to formulation NP-GSH-Rh was performed by an indirect method that involves hybridization of the sulfhydryl group with Ellman's reagent (DTNB, 5,5′-dithiobis-(2-nitrobenzoic acid). DTNB is used for quantitating free sulfhydryl groups in solution with the reaction involved depicted in Fig. 1 in which a yellow-coloured product (TNB, 5-thio-2-nitrobenzoic acid) is released when DTNB reacts with sulfhydryl groups. This yellow-coloured product can be quantified by spectrophotometry.

Calibration curves were prepared in triplicate using GSH solutions at concentrations of 2, 4, 20, 40, 60, 80, and 100 μg/mL. Subsequently, 1 mL of each solution was reacted for 30 min with 3 mL of DTNB that prepared in PBS at pH 7.4 is ionized ($DTNB^{2-}$). The resulting theoretical

Table 1
Nanoparticle (NPs) formulations developed. Rh-B: rhodamine B, GSH: glutathione, PHE2: phenylalanine dipeptide.

Formulation	PLGA 502 (mg)	Peptide/mg	Rh-B (mg)
NP-Rh	50	–	2.5
NP-GSH-Rh	50	GSH/2.0	2.5
NP-PHE2-Rh	50	PHE2/2.0	2.5

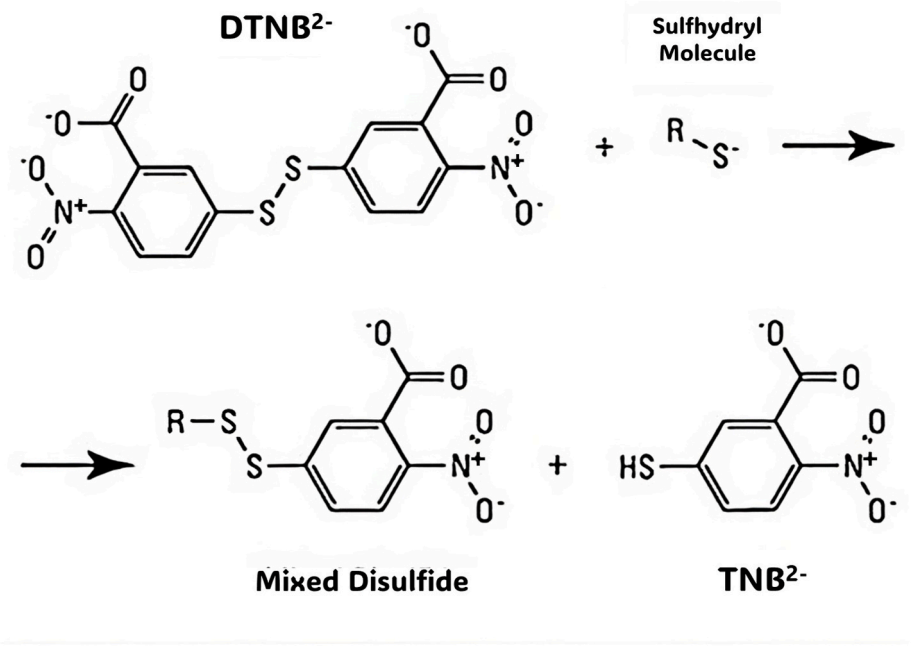

Fig. 1. Reaction for the quantification of glutathione (GSH) bound to formulation NP-GSH-Rh.

GSH concentrations were 0.5, 1.5, 8, 15, 20, and 25 μg/mL.

The TNB^{2-} dianione obtained was quantified by UV/Vis spectrophotometry (Jasco International Co., Ltd., Tokyo, Japan) at a wavelength of 410 nm.

2.5. Functionalization of nanoparticles with phenylalanine dipeptide

Phenylalanine dipeptide (PHE2) was linked from its amine terminal group to the carboxylic terminal group of the PLGA of the NPs by a carbodiimide reaction adapted from the protocol described by Constantino et al. [12]. For this, 0.5 mL of 0.1 M MES buffered solution at pH 4.7 were added to 55 mg of formulation NP-Rh suspended in 1 mL of distilled water. To this solution 50 mg of NHS were added. Then, 150 mg of EDC dissolved in 2.5 mL of 0.1 M MES buffered solution were added. The NPs suspension was maintained under magnetic stirring for 1 h and thereafter centrifuged at 20,150 g for 25 min to remove MES buffer and all unreacted reagents.

Then, the recovered NPs were suspended in 2.5 mL of PBS at pH 7.4. Meanwhile, a PHE2/PBS solution (0.8 mg/mL) was prepared. From this solution, 2.5 mL were added to the previous NPs-PBS suspension with the resulting mixture magnetically stirred for 2 h to ensure that the reaction was completed. Finally, the NPs were recovered by centrifugation (20,150 g, 30 min) and freeze-dried suspended in 1 mL of a 1.5 % sucrose solution (cryoprotectant). The PBS obtained from the supernatant of the NPs was analyzed for quantification of PHE2.

Fig. 2 shows the reaction involved in the functionalization of formulation NP-Rh with PHE2.

2.6. Determination of PHE2 bound to the nanoparticles

Quantification of PHE2 bound to the surface of NPs was carried out indirectly. For this, the supernatant containing the unbound peptide was analyzed by the method described by Neurauter et al. [13] adapted to our experimental conditions [14]. The chromatographic analysis was performed in a Jasco HPLC (Jasco International Co., Ltd., Tokyo, Japan) equipped with a fluorescence detector (Jasco FP-4025, Jasco

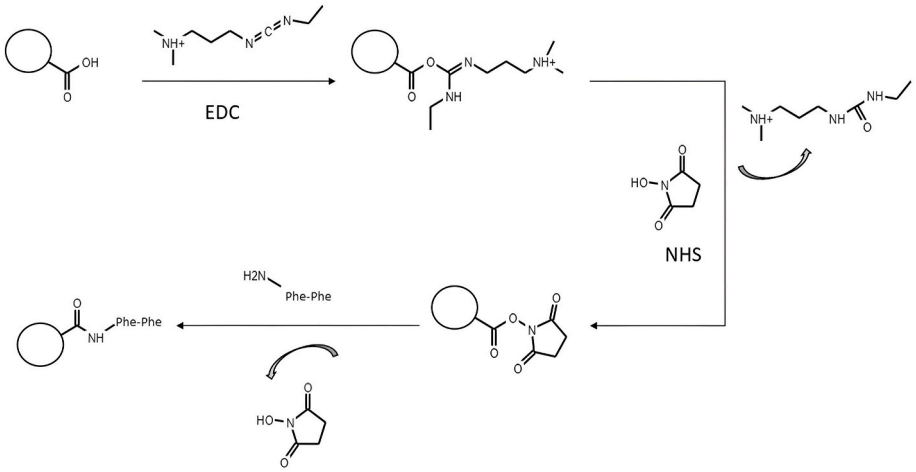

Fig. 2. Reaction involved in the functionalization of formulation NP-Rh with phenylalanine dipeptide (PHE2).

International Co., Ltd., Japan). The average calibration curve used for this quantification (50, 100, 250, 300, 400 and 500 μg/mL) was y = 35447 + 638.32x (R^2 = 0.9991) where y is the peak area and x the concentration of PHE2.

2.7. Characterization of nanoparticles

2.7.1. Morphology

Dynamic light scattering was used to determine the polydispersity index (PDI), size distribution and mean diameter of the NPs by using a Zetatrac® Ultra 3500 system (Microtrac MRB, Montgomeryville, USA). The mean diameter was expressed as volume diameter.

The NPs were also examined by scanning electron microscopy (SEM) (Jeol JSM 7600F, Jeol Ltd., Tokyo, Japan) to analyse shape and surface morphology. For SEM analysis the cryoprotectant was firstly eliminated by suspending the NPs in MiliQ-water and centrifuging at 20,150 g for 20 min with this step repeated three times. Then, a drop of the NPs suspension was added to a coverslip adhered to a stub and maintained in a desiccator for 24 h. Finally, the samples were coated with a thin layer of colloidal gold applied through a cathodic vacuum evaporator.

2.7.2. Zeta potential

Determination of zeta potential was carried out by Laser-Doppler anemometry using a Malvern Zetasizer Nano S® (Malvern Panalytical, Ltd., Malvern, U.K.). For this, 5 mg of each NPs formulation were suspended in 50 mL of distilled water and stirred for 1 min. Zeta potential measurements were carried out by placing the resulting aqueous dispersion with a concentration of 100 μg/mL of NPs into a capillary cell (Cell Enhances Capillary®, Malvern Panalytical, Ltd., Malvern, U.K.). Zeta potential measurements were performed in triplicate.

2.7.3. Encapsulation efficiency

Encapsulation efficiency (EE%) of Rh-B within PLGA NPs was determined by dissolving 10 mg of each formulation in 1 mL of DCM. Then, 15 mL of methanol were added to the previous solution, mixed, and centrifuged at 7750 g for 5 min. The supernatant (5 mL) was analyzed by spectrophotometry at 555 nm.

For this quantification a spectrophotometric method was developed using concentrations of 0.5, 1, 2, 3, 4 and 5 μg/mL of Rh-B in methanol. The average equation obtained was y = 0.0098 + 0.1992x (R^2 = 0.9998), where y is the absorbance and x the concentration of Rh-B.

2.7.4. In vitro release studies

In vitro release of Rh-B from the NPs was carried out in a Memmert WB22 water bath (Memmert GmbH, Büchenbach, Germany) at 37 ± 0.1 °C and constant agitation (100 rpm). For this, 20 mg of NPs were weighed, placed in Eppendorf tubes, and suspended in 4 mL of PBS solution at pH 7.4. At regular time intervals (1, 2, and 6 h) samples were centrifuged, the supernatant removed and filtered through 0.45 μm PVDF filters (Teknokroma Analítica, S.A., Barcelona, Spain). Quantification of Rh-B was performed by spectrophotometry at 555 nm. All release tests were carried out in triplicate.

For the quantification of Rh-B in PBS a spectrophotometric method was developed which was linear within the following concentration range: 0.5, 1, 2, 3, 4, and 5 μg/mL. The average calibration curve obtained was y = 0.0021 + 0.227x (R^2 = 0.9997) where y is the absorbance and x the concentration of Rh-B. The limit of detection (LOD) was 0.156 μg/mL and the limit of quantification (LOQ) was 0.449 μg/mL.

2.8. Biodistribution studies

For the biodistribution studies male Wistar rats (Harlan France SARL, Gannat, France) weighing 220–270 g were used. Animals were housed with controlled temperature and 12h:12h light:dark cycles, observed daily and fed with commercial pelleted diet and water ad libitum All animal procedures were approved by the Ethics Committee on Animal Experimentation (Universidad Complutense de Madrid, UCM) and the regional authorities (Madrid Region, PROEX 14/18). All procedures complied with the European Community Council Directive (010/63/UE). Efforts were made to minimize the number of animals used and their suffering.

Animals were divided into four experimental groups.

- Group 1 (n = 4) received saline solution.
- Group 2 (n = 6) received formulation NP-GSH-Rh.
- Group 3 (n = 6) received formulation NP-PHE2-Rh.
- Group 4 (n = 6) received formulation NP-Rh.

The NPs were suspended in saline at a concentration of 25 mg/mL. The volume given was adjusted by weight, utilizing 0.5 mL as a reference volume for the average animal weight. The suspension was injected into the rat tail vein using a 30-gauge needle. Finally, the rats were anesthetized with isoflurane. Half of the animals within each group were sacrificed at time 1 h and the other half at 2 h.

Biodistribution analysis of the NPs formulations was conducted by measuring the fluorescence of Rh-B in various organs (liver, kidneys, spleen and lungs) according to the method described by Marcianes et al. [15] and adapted to our experimental conditions. After sacrifice, the liver, lungs, kidneys, and spleen were extracted from all animals. The extracted organs were frozen in dry ice and kept at −80 °C until analysis.

Quantification of Rh-B was performed as follows: each organ was weighed and a portion (1.5 ± 0.1 g) was homogenized in 5 mL of DCM using a turbine. After 1 h homogenization protected from light exposure, the mixture was centrifuged at 12,400 g for 10 min to extract all Rh-B content. Rh-B was quantified by measuring its fluorescence in a Varian Cary Eclipse fluorescence spectrophotometer (Agilent Technologies, Madrid, Spain). Excitation and emission wavelengths were set at 553 nm and 627 nm, respectively. The fluorescence intensity from non-treated animals was used as a background signal (negative controls) to discard tissue autofluorescence. The amount of Rh-B was expressed as ng of Rh-B/g tissue. As the different formulations presented different drug loadings (DL), the results were normalized for the same dose of Rh-B.

The calibration curve was linear with the concentration range 1–400 ng/mL resulting in the following average equation: y = 0.0011 + 0.1744x (R^2 = 0.9987).

2.9. Passage of NPs through the BBB

The passage of NPs through the BBB was studied after i.v. administration to male Wistar rats. For this, once animals were sacrificed, brains were removed and divided into both hemispheres. The right hemisphere was used to determine the NPs that crossed the BBB. This study was carried out following the protocol previously described.

2.10. Regional brain distribution

The left hemisphere was used to study the distribution of NPs in different areas of the brain. For this, the hemisphere was sectioned into 25 μm slices corresponding to hippocampus, cortex and substantia nigra. The slices were embedded for 24 h in DAPI solution (4',6-diamidino-2-phenylindole) (125 ng/mL) [16] and analyzed by confocal microscopy in a Leica microscope (Leica Microsystems GmbH, Wetzlar, Germany) at 545 nm excitation and 570 nm emission wavelengths [17]. ImageJ was the software used to quantify the intensity of Rh-B fluorescence in the samples [18]. Negative control rats were used to discard tissue autofluorescence.

2.11. Brain tissue integrity

To determine if the administration of NPs produced brain tissue damage, NISSL staining was performed. NISSL staining was carried out by immersing the samples fixed to a sample holder in a cresyl violet

solution for 30 min. Then, samples were washed, using increasing concentrations of ethanol for 2 min. Finally, to ensure that samples were dehydrated, two 5-min washes were carried out in xylene.

Images were acquired on a Leica model DM2000 LED microscope coupled to a digital camera (Leica DFC425 for colour captures of cresyl violet stains) (Leica Microsystems GmbH, Wetzlar, Germany). Images captured using Leica LAS software were subsequently exported in jpeg format.

2.12. Statistical analysis

Results are expressed as mean standard deviation. Multifactorial ANOVA tests were performed using the Statgraphics 19-X64® Centurion software (Statgraphics Technologies, Inc., The Plains, USA). A p-value <0.05 was considered statistically significant.

3. Results and discussion

Surface functionalization of NPs can be used for different purposes which include improving their passage through the BBB [19]. For this, attachment of ligands to the surface of NPs can facilitate their access to the CNS.

Several endogenous transporters facilitate the access of essential substances to the brain, such as glucose, galactose, amino acids, nucleosides, purines, amines or vitamins. Among the transporters expressed in the BBB are the glucose transporter GLUT-1 [20] and the L-type amino acid transporter 1 (LAT-1) [21].

LAT-1 is expressed in brain capillary endothelial and parenchymal cells forming the BBB being specially interesting for targeted drug delivery to the brain due to its tissue-specific expression profile [22,23]. LAT-1, an isoform of the amino acid transport system L, transports large neutral amino acids with branched or aromatic side chains, such as phenylalanine, valine, methionine and tyrosine, among others, with phenylalanine being one of the amino acids showing higher affinity for the transporter [24].

It has been indicated that LAT-1 is expressed as much as 100-fold greater levels in the BBB compared to other tissues, thereby resulting in an interesting approach for delivering amino acid-mimicking drugs to the CNS [25].

Notably, several drugs on the market reach the brain via this transporter, such as baclofen, gabapentin and the antiparkinsonian drug L-DOPA [26].

Glutathione (GSH) is an essential endogenous tripeptide involved in intracellular metabolite detoxification. It is a high hydrophilic compound negatively charged at physiological pH unable to penetrate cell membranes thereby requiring a carrier-mediated transporter (GSH transporter). A study performed by Kannan et al. [27] demonstrated the existence of Na + -dependent GSH transporters localized at the luminal apical membrane of brain endothelial cells as well as Na + -independent GSH transporters in an in vitro BBB model developed in human cerebral microvascular endothelial cells (HCEC).

In our work two ligands that can be substrates for these transporters have been selected in order to facilitate the passage of polymeric NPs to the CNS: glutathione (GSH) and phenylalanine dipeptide (PHE2).

Rhodamine B (Rh-B) is a well-known P-glycoprotein (P-gp) substrate used in our work as fluorescent tracer as it is unable to freely cross the BBB. PLGA was selected as polymer due to its adequate characteristics such as biocompatibility and biodegradability. PLGA is used in most controlled release systems approved by the FDA [28] and exhibits the ability to partially cross the BBB [29]. Different studies have shown that surface functionalization of PLGA NPs with surfactants such as poloxamer 407, P188, cholic acid or tween 80 can facilitate the uptake of NPs by brain cells thereby leading to better brain targeting [30,31].

Binding these ligands to the surface of NPs can be achieved by different approaches. For instance, ligands can be attached to the polymer (PLGA) before elaborating the NPs or the ligand can be attached to the surface of NPs already loaded with the active ingredient [12]. Both methods have advantages and drawbacks. The union of ligands directly to the surface of NPs loaded with the active ingredient is easier and avoids the internalization of the ligand towards the core of the particles during preparation. However, surface functionalization of nanoparticles involves an extended period of time needed to allow enough contact between the NPs and the reagents. During this time if the encapsulated drug is not lipophilic enough, a significant loss of the drug can occur. In a study conducted by our research team, morin-loaded PLGA NPs were functionalized with phenylalanine dipeptide, which resulted in improved passage through the BBB. Functionalization was carried out directly on the polymer before preparing the NPs. With this formulation we were able to observe that part of the dipeptide PHE2 was located towards the interior of the NPs [32].

Taking into consideration these results, in this work phenylalanine dipeptide (PHE2) and glutathione (GSH) have been used to functionalize the surface of rhodamine B-loaded PLGA NPs.

In the present study binding GSH and PHE2 to the surface of rhodamine B loaded PLGA NPs was achieved by activating the -COOH groups of PLGA with 1-ethyl-3-(3-dimethylaminopropyl) carbodiimide (EDC) and N-hydroxysuccinimide (NHS) in MES medium. The conjugation efficiency obtained was 64.5 ± 10.8 % for GSH and 21.7 ± 112.3 % for PHE2. Although the results obtained with glutathione are better, both formulations were suitable for our purposes.

Binding of these ligands could lead to modifications in the characteristics of the NPs. Table 2 shows the results obtained for all Rh-B formulations. In the table, results obtained for non-loaded functionalized NPs are also included for comparison reasons (NP-0).

For NPs to be able to reach the CNS particle sizes should be around 100–250 nm [33]. In our case, the method used for the elaboration of NPs resulted in particle sizes smaller than 200 nm, thereby being adequate for this purpose.

Gao and Jiang [8] prepared methotrexate-loaded polybutylcyanoacrylate NPs coated with polysorbate 80 to study the influence of size on their ability to cross the BBB. NPs were prepared with mean sizes of 70, 170, 220, and 345 nm. The authors found that 70-nm NPs coated with polysorbate 80 delivered the drug more efficiently into the brain with no significant differences observed among the other three size ranges. The authors attributed this fact to an endocytosis process which is favoured by NPs with sizes <100 nm. In our case, mean particle sizes ranged from 176.4 nm to 195.47 nm, which allowed us to evaluate the effect of surface functionalization on the passage of NPs through the BBB.

PDI (polydispersity index) is a measure of the heterogeneity of a sample based on its size. This parameter evaluates the size distribution, but also the possible aggregation/agglomeration of the sample during isolation or analysis, with PDI values < 0.5 being generally accepted [34]. In our case, all PDI values were <0.4 (Table 2).

Span correlates with the width of particle size distribution. The smaller the span value is, the narrower the particle size distribution is. In our case, all span values obtained were <0.9 indicating homogeneous particle size populations.

Nanoparticles exhibiting zeta potential values higher than +30 mV or lower than −30 mV present lower tendency for aggregation thereby being more stable. When particles are neutral or negatively charged

Table 2
Mean particle size (±SD), PDI (polydispersity index), Span and Z potential values (±SD) obtained for all formulations.

Formulation	Particle size ± SD (nm)	PDI	Span	Z potential ± SD (mV)
NP-0	176.4 ± 13.45	0.22	0.68	−24,93 ± 1.38
NP-Rh	187.67 ± 6.92	0.25	0.71	−21.75 ± 0.48
NP-GSH	191.33 ± 10.69	0.20	0.78	−27.61 ± 0.71
NP-GSH-Rh	192.77 ± 1.44	0.19	0.68	−26.88 ± 0.69
NP-PHE2	195.47 ± 12.99	0.18	0.63	−20.03 ± 0.21
NP-PHE2-Rh	190.66 ± 4.67	0.31	0.83	−18.46 ± 0.74

longer circulating times and fewer side-effects are described than positively-charged nanoparticles [35]. The mean Z potential value obtained for blank PLGA NPs (NP-0) was −24,93 ± 1.38 mV, similar to those obtained in other studies [15,17]. The Z potential significantly increased with the presence of PHE2 and slightly decreased when the NPs were functionalized with GSH. However, these variations did not modify the characteristics of the particles.

Fig. 3 shows photomicrographs obtained by SEM corresponding to formulations NP-GSH-Rh and NP-PHE2-Rh.

SEM microphotographs showed that both formulations exhibited smooth and rigid surfaces with homogeneous sizes. Aggregates were not observed that could hinder i.v. administration of the particles. These results agree with those obtained by means of laser diffraction analysis.

Table 3 summarizes the mean results obtained for the encapsulation efficiency of Rh-B within the NPs along with drug loading and mean cumulative amount of Rh-B released from the NPs at 1 h and 2 h.

As it can be seen low EE values were obtained for all formulations, taking into consideration the hydrophilic nature of Rh-B, and particularly for the NPs functionalized with PHE2. Preliminary experiments carried out increasing the initial amount of Rh-B during the preparation of NPs resulted in an interaction between Rh-B and PLGA that led to a modification of the polymer characteristics. From those results, a 2.5 % concentration of Rh-B was considered enough to perform the *in vivo* biodistribution studies. This means that although low EE of Rh-B within the NPs was obtained it was considered adequate for our purposes.

These low EE values are probably due to the functionalization process which requires of long contact times between the NPs and the MES and PBS media resulting in the release (loss) of the fluorescent tracer during this process.

The differences obtained in the EE values among the NPs formulations (Table 3) made it necessary to normalize the results obtained in the *in vivo* biodistribution studies.

In vitro release of Rh-B from the NPs was studied for the only purpose of getting an approximate idea of whether there might be a correlation between the in vitro and *in vivo* behavior of the formulations. The release tests were carried out up to 6 h with intermediate samples taken at 1 h and 2 h as sampling times established to study *in vivo* the passage of NPs through the BBB and their brain distribution were 1 h and 2 h. Nevertheless, at the 6-h time point the mean amounts of Rh-B released were 256.10 ± 2.0, 220.73 ± 10.49 and 55.6 ± 0.40 μg/100 mg NPs for formulations NP-Rh, NP-GSH-Rh and NP-PHE2-Rh, respectively. When analyzing the *in vivo* results obtained, it must be taken into account that partial release of Rh-B may occur before crossing the BBB, indicating that a portion of the encapsulated tracer may be lost before the NPs cross the BBB. In this regard it must be stated that previous studies carried out by our research team showed that the greatest passage of PLGA NPs through the BBB occurred within the first 30 min after administration [15].

From the results obtained with formulation NP-GSH-Rh (Table 3) it can be observed that the functionalization process produced a decrease in the release rate of Rh-B from the NPs. This may be due to the fact that the functionalization process creates an additional layer on the surface of the nanosystems thereby modifying the release rate of the encapsulated tracer [36]. The same was observed with formulation NP-PHE2, but in this case the very low loading of Rh-B also contributed to the decrease in the release rate.

Table 3
Mean results (±SD) of encapsulation efficiency, drug loading and amounts of Rh-B (±SD) released from the NPs at 1 h and 2 h.

Formulation	EE (%) ± SD	DL (μg/100 mg NPs) ± SD	Mean amounts of Rh-B (μg/100 mg NPs) ± SD	
			1h	2h
NP-Rh	7.7 ± 0.3	357.3 ± 17.3	159.6 ± 1.3	223.8 ± 1.8
NP-GSH-Rh	8.8 ± 0.6	408.4 ± 8.4	137.6 ± 3.3	192.9 ± 7.3
NP-PHE2-Rh	2.3 ± 0.2	108.9 ± 11.4	31.0 ± 3.3	49.8 ± 0.5

Biodistribution studies were conducted 1 h and 2 h after i.v. administration of the NPs formulations to male Wistar rats by quantifying the amount of Rh-B in liver, kidneys, spleen, and lungs. Due to the different amounts of Rh-B encapsulated within each formulation it was necessary to normalize the results. Firstly, biodistribution of the tracer (Rh-B) in the organs was compared. Fig. 4 shows the results obtained.

During the first hour the formulation functionalized with GSH (NP-GSH-Rh) was more prominently present in the liver in comparison to formulations NP-PHE2-Rh and NP-Rh but the amount of Rh-B from the NPs functionalized with phenylalanine dipeptide (NP-PHE2-Rh) significantly increased after 2 h reaching higher mean value than that obtained for formulation NP-GSH-Rh (Fig. 4).

Regarding the presence of the tracer in the spleen at both time points, the values corresponding to the both functionalized formulations (NP-GSH-Rh and NP-PHE2-Rh) were significantly higher than those obtained for non-functionalized NPs (NP-Rh). In the lungs the values obtained in the first hour were significantly different for the three formulations assayed. At 1 h-time point formulation NP-GSH-Rh showed the highest affinity for the lungs whereas this result was reversed after 2 h, time at which formulation NP-PHE2-Rh exhibited the highest affinity. For non-functionalized NPs (NP-Rh) similar values were obtained at both time points (Fig. 4).

Lastly, the quantities of Rh-B in the kidneys at both time points were very low for all formulations in comparison to the amounts found in the other organs.

The presence of ligands (GSH and PHE2) may modify the biodistribution of NPs, especially in the spleen. Some nanosystems tend to target organs taken up by phagocytic cells, such as macrophages in the spleen. The biodistribution results obtained seem to suggest that the process of functionalization could stimulate phagocytosis and migration of NPs towards these organs which would explain the higher presence of functionalized NPs in phagocytic organs, with non-functionalized NPs

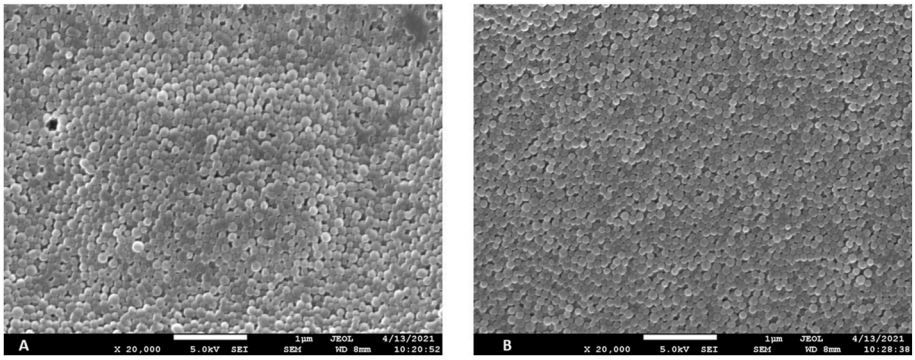

Fig. 3. Photomicrographs obtained by SEM of formulations (A) NP-GSH-Rh and (B) NP-PHE2-Rh.

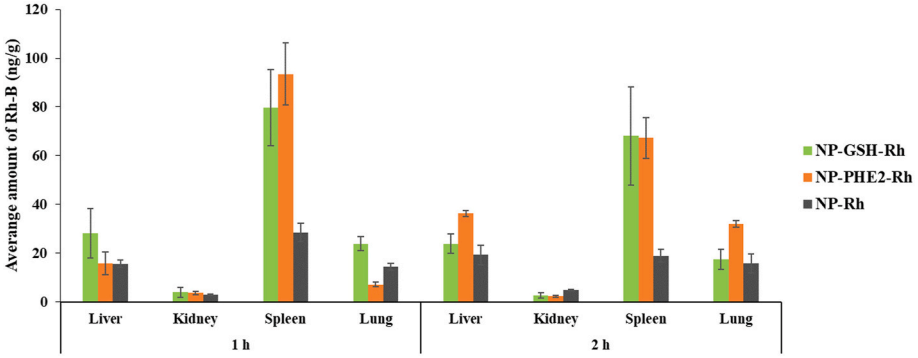

Fig. 4. Mean amounts (±SD) of Rh-B in liver, kidneys, spleen, and lungs after the administration to male Wistar rats of Rh-B loaded PLGA NPs (functionalized and non-functionalized formulations). Rh-B: rhodamine B.

being more rapidly eliminated.

Surface functionalization of polymeric NPs is a key approach when aiming to efficiently cross the BBB. Specific ligands can be conjugated onto PLGA NPs to promote recognition by receptors on the endothelial cells. Peptides, which are short chains of amino acids, have demonstrated significant potential as conjugating ligands to facilitate BBB transcytosis. Moreover, functionalization with peptides is cost-efficient exhibiting reduced immunogenicity [37], and versatility for conjugation [38].

In our study glutathione (GSH) and phenylalanine dipeptide (PHE2) were selected as ligands. GSH can use the glutathione transporters to cross the BBB and the dipeptide phenylalanine which contains aromatic groups, may use the L-type amino acid transporter 1 (LAT-1). Both transporters are highly expressed in the BBB compared to other tissues [39].

Fig. 5 shows the average amounts of Rh-B detected in the brain 1 h and 2 h after the administration of all NPs formulations to male Wistar rats.

At both time points functionalized formulations NP-GHS-Rh and NP-PHE2-Rh showed statistically significant higher amounts of Rh-B than non-functionalized NPs (NP-Rh) which can be clearly related to the greater passage of functionalized NPs across the BBB.

Regarding formulation NP-PHE2-Rh a significant reduction of the amount of Rh-B was obtained at time 2 h that could be related to the very low loading of the tracer within this formulation and its rapid release. Rhodamine is a well-known P-gp substrate that once released from the NPs in the brain it will be readily expelled [21]. For this reason and taking into consideration the low EE obtained for formulation NP-PHE2-Rh, 2 h after the administration very low levels of Rh-B were detected in the brain. On the other hand, it must be taken into account that phenylalanine is an amino acid with a gradient favourable to entry the brain tissue, but not to be expelled.

Nevertheless, the average amounts of Rh-B obtained for both functionalized formulations were higher than that of non-functionalized NPs at both time points.

GSH transporter is highly expressed at the BBB level [40,41] playing an important antioxidant role as protects cells against reactive oxygen and nitrogen species [42].

In view of the results obtained, the exploitation of the BBB's natural transport mechanisms, such as the GSH or PHE2 transporters represents an interesting approach for enhancing the delivery of therapeutic agents to the CNS.

Studying the distribution of NPs within different brain regions may be highly interesting to facilitate the access of drugs encapsulated within these nanosystems, and when aiming to treat pathologies affecting the CNS. Moreover, regional biodistribution studies allow evaluating the effect of NPs functionalization on their brain distribution. In our study, the fluorescent compound was detected and quantified after the administration of all Rh-B loaded NPs (NP-Rh, NP-GSH-Rh, NP-PHE2-Rh) in the substantia nigra (SN), cortex (COR) and hippocampus (HIP) (Fig. 6).

The impact of surface modification on the regional distribution of nanoparticles in the brain remains a challenge. In our study the results obtained 1 h after the administration of the NPs revealed that the highest intensity of fluorescence was detected in the hippocampus, followed by the cortex and substantia nigra (Fig. 6). Cook et al. [9] suggested that differences between brain regions might be related to differences in blood flow. In our case both functionalized formulations led to significantly higher values of fluorescence intensity in the hippocampus when compared to the other regions (COR and SN). At this time point comparison of the formulations in the cortex region of the brain did not show any significant differences between functionalized and

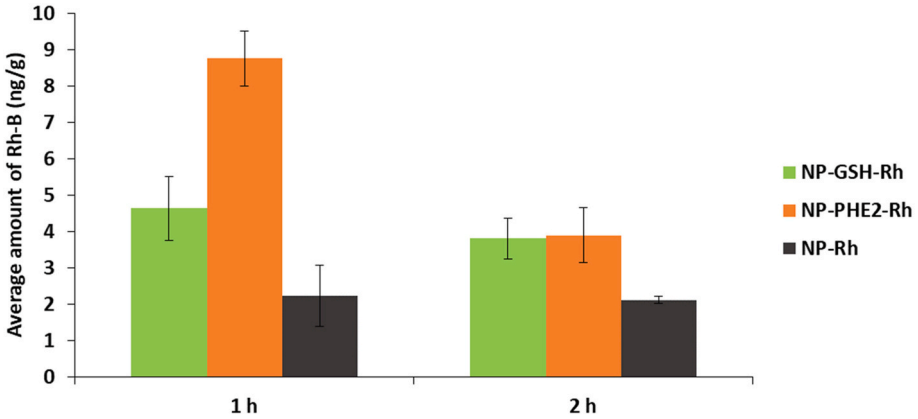

Fig. 5. Average amounts (±SD) of Rh-B detected in the brain 1 h and 2 h after the administration of all NPs formulations to male Wistar rats.

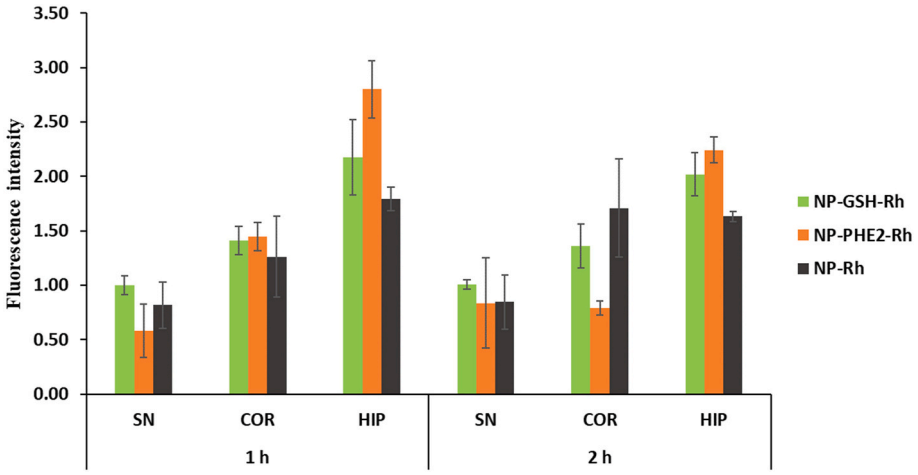

Fig. 6. Average values (±SD) of intensity of fluorescence obtained in the substantia nigra (SN), cortex (COR) and hippocampus (HIP) at times 1 h and 2 h after the administration of formulations NP-Rh, NP-GHS-Rh and NP-PHE2-Rh.

non-functionalized NPs. In the substantia nigra formulation NP-PHE2-Rh showed low fluorescence intensity values but without statistically significant differences when compared to the other formulations (Fig. 6).

The results obtained in the first hour could be attributed to the fact that the BBB is not equally restrictive throughout the CNS. In those areas where its structure is more permissive, passive diffusion and the interventions of LAT1 transporters would allow faster passage of NPs, while in other more isolated areas such as the substantia nigra, passive diffusion will probably be less effective, giving priority to transport through slower channels.

When analyzing the results obtained 2 h after administering the NPs it can be observed that both functionalized formulations (NP-GSH-Rh and NP-PHE2-Rh) led to higher fluorescence intensity values in hippocampus that were statistically significant when compared to non-functionalized NPs (Fig. 6). These results are of special interest taking into consideration that the presence of the NPs in the brain after 2 h counteracts the efflux activity of P-glycoprotein, thereby remaining in the area for a longer period of time where the therapeutic effect may be exerted. Although a reduction of fluorescence was achieved in this area at 2 h in comparison with 1 h however, the values obtained in hippocampus were still higher than those in the cortex and substantia nigra.

At this time point (2 h) the results obtained in substantia nigra were similar for the three formulations (NP-GSH-Rh, NP-PHE2-Rh and NP-Rh) also indicating that the NPs remained in this area. At the cortex level both NP-Rh and NP-GSH-Rh formulations showed similar intensity of fluorescence that was markedly reduced for formulation NP-PHE2-Rh.

Therefore, from these results it can be stated that 2 h after the administration of functionalized PLGA NPs (NP-GSH-Rh and NP-PHE2-Rh) statistically significant higher intensity of fluorescence values were obtained in the hippocampus when compared to non-functionalized NPs.

From our results and in concordance to those obtained by Gao and Jiang [8] denote that particle sizes between 170 and 340 nm have less impact on their ability to cross the BBB than the functionalization process.

When treating pathologies affecting the CNS the administration of drugs encapsulated within polymeric NPs may be a very interesting approach to gain access to different brain regions. Hippocampus is a complex brain structure located in the temporal lobe that plays a major role in learning and memory but also in spatial navigation, emotional behavior and regulation of hypothalamic functions [43,44]. Hippocampal lesions generally cause severe difficulties in the formation of new memories, with long-term memory being the most affected. The most common pathologies affecting the hippocampus include neurodegenerative diseases such as Alzheimer's disease and frontotemporal dementia, pathologies for which there is currently no cure. Therefore, functionalization of NPs could be of great interest for treating these pathologies.

Finally, to assess if the presence of NPs damaged brain tissue NISSL-staining was performed on the hippocampus, cortex and substantia nigra. Images of the results obtained are depicted in Fig. 7.

As it can be seen no structural damage was caused by the administration of the NPs formulations in any of the brain areas analyzed (hippocampus, cortex, and substantia nigra). These results together with the improvement of the access of functionalized NPs to the hippocampus with ligands that can be specifically recognized by transporters expressed at the BBB level such as GSH and LAT-1 are very promising for future therapeutic applications taking into consideration the need to circumvent the physical barrier that the BBB represents for the access drugs to the brain at high concentrations which still remains a major challenge to improve current therapies of CNS pathologies.

4. Conclusions

Surface functionalization of PLGA nanoparticles with glutathione or phenylalanine (formulations NP-GSH-Rh and NP-PHE2-Rh) favoured their passage across the BBB. Glutathione transporter and L-type amino acid transporter 1 (LAT-1) which are highly expressed at the BBB level may be involved in this passage. Regarding the distribution of the nanoparticles in different areas of the brain both functionalized formulations (NP-GSH-Rh and NP-PHE2-Rh) predominantly reached the hippocampus with differences being statistically significant when compared to non-functionalized NPs and remained in this area for at least 2 h where the therapeutic effect may be exerted specially in pathologies affecting this area such as Alzheimer's disease and frontotemporal dementia. No structural damage was caused by the nanoformulations in the hippocampus, cortex or substantia nigra. These promising results must be considered as preliminary efforts that require further investigations to select the most adequate ligand for a specific biological target, especially when aiming to treat neurodegenerative diseases for which there is currently no cure. For this future research will firstly involve evaluating the performance of both functionalized formulations in an animal model of Alzheimer's disease in which the BBB is altered.

CRediT authorship contribution statement

Mario Alonso: Methodology, Investigation, Data curation. **Emilia**

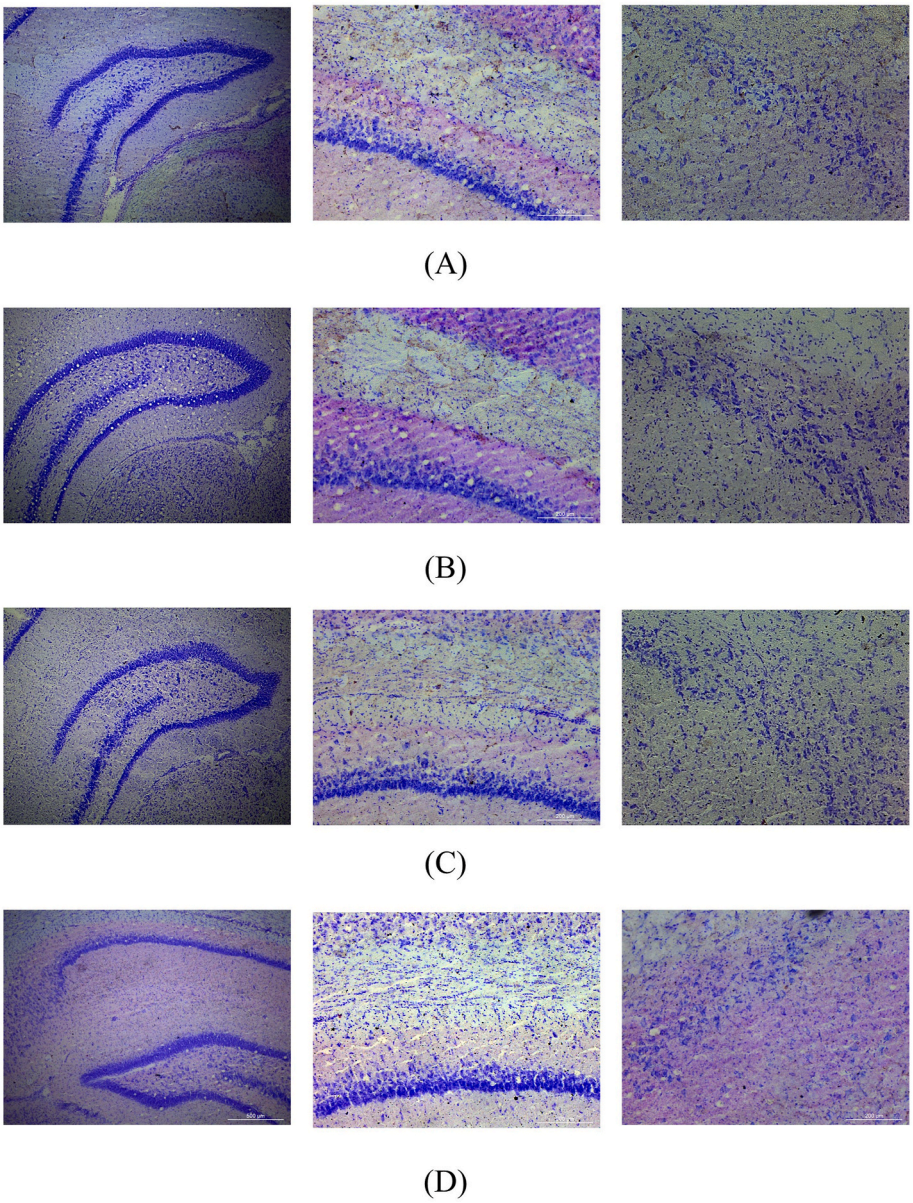

Fig. 7. Images of hippocampus (left), hippocampus and cortex (middle) and substantia nigra (right) obtained at 2 h for (A) negative control group, (B) NP-Rh, (C) NP-GSH-Rh, and (D) NP-PHE2-Rh.

Barcia: Writing – review & editing, Funding acquisition, Formal analysis, Data curation, Conceptualization. **Sofía Negro:** Writing – original draft, Methodology, Funding acquisition, Formal analysis, Data curation. **Nicola Paccione:** Investigation. **Mahdieh Rahmani:** Investigation. **Consuelo Montejo:** Investigation, Data curation. **Luis García-García:** Investigation, Data curation. **Ana Fernández-Carballido:** Writing – original draft, Supervision, Methodology, Formal analysis, Conceptualization.

Declaration of competing interest

The authors declare that they have no known competing financial interests or personal relationships that could have appeared to influence the work reported in this paper.

Acknowledgements

This work was partially supported by Complutense University of Madrid (UCM) research group "Formulation and Bioavailability of New Drugs" (funder UCM, funding number 910939).

Data availability

Data will be made available on request.

References

[1] F.L. Cardoso, D. Brites, M.A. Brito, Looking at the blood–brain barrier: molecular anatomy and possible investigation approaches, Brain Res. Rev. 64 (2010) 328–363, https://doi.org/10.1016/j.brainresrev.2010.05.003.
[2] R.G.R. Pinheiro, A.J. Coutinho, M. Pinheiro, A.R. Neves, Nanoparticles for targeted brain drug delivery: what do we know? Int. J. Mol. Sci. 22 (2021) 11654 https://doi.org/10.3390/ijms222111654.
[3] S. Chen, C. Jin, R. Ohgaki, M. Xu, H. Okanishi, Y. Kanai, Structure–activity characteristics of phenylalanine analogs selectively transported by L-type amino acid transporter 1 (LAT1), Sci. Rep. 14 (2024) 4651, https://doi.org/10.1038/s41598-024-55252-w.
[4] V. Ceña, P. Játiva, Nanoparticle crossing of blood–brain barrier: a road to new therapeutic approaches to central nervous system diseases, Nanomedicine. 13 (2018) 1513–1516, https://doi.org/10.2217/nnm-2018-0139.

[5] D.S. Hersh, A.S. Wadajkar, N.B. Roberts, J.G. Perez, N.P. Connolly, V. Frenkel, J. A. Winkles, G.F. Woodworth, A.J. Kim, Evolving drug delivery strategies to overcome the blood brain barrier, Curr. Pharm. Des. 22 (2016) 1177–1193, https://doi.org/10.2174/1381612822666151221150733.

[6] J.E. Preston, N. Joan Abbott, D.J. Begley, Transcytosis of macromolecules at the blood-brain barrier, Adv. Pharmacol. 71 (2014) 147–163, https://doi.org/10.1016/bs.apha.2014.06.001.

[7] Y. Guo, H. Lee, Z. Fang, A. Velalopoulou, J. Kim, M.B. Thomas, J. Liu, R. G. Abramowitz, Y. Kim, A.F. Coskun, D.P. Krummel, S. Sengupta, T.J. MacDonald, C. Arvanitis, Single-cell analysis reveals effective siRNA delivery in brain tumors with microbubble-enhanced ultrasound and cationic nanoparticles, Sci. Adv. 7 (2021) eabf7390, https://doi.org/10.1126/sciadv.abf7390.

[8] K. Gao, X. Jiang, Influence of particle size on transport of methotrexate across blood brain barrier by polysorbate 80-coated polybutylcyanoacrylate nanoparticles, Int. J. Pharm. 310 (2006) 213–219, https://doi.org/10.1016/j.ijpharm.2005.11.040.

[9] R.L. Cook, K.T. Householder, E.P. Chung, A.V. Prakapenka, D.M. DiPerna, R. W. Sirianni, A critical evaluation of drug delivery from ligand modified nanoparticles: confounding small molecule distribution and efficacy in the central nervous system, J. Contr. Release 220 (2015) 89–97, https://doi.org/10.1016/j.jconrel.2015.10.013.

[10] J. Hammond, B.A. Maher, I.A.M. Ahmed, D. Allsop, Variation in the concentration and regional distribution of magnetic nanoparticles in human brains, with and without Alzheimer's disease, from the UK, Sci. Rep. 11 (2021) 9363, https://doi.org/10.1038/s41598-021-88725-3.

[11] J. Kreuter, Drug delivery to the central nervous system by polymeric nanoparticles: what do we know? Adv. Drug Deliv. Rev. 71 (2014) 2–14, https://doi.org/10.1016/j.addr.2013.08.008.

[12] L. Constantino, F. Gandolfi, G. Tosi, F. Rivasi, M.A. Vandelli, F. Forni, Peptide-derivatized biodegradable nanoparticles able to cross the blood-brain barrier, J. Contr. Release 108 (2005) 84–96, https://doi.org/10.1016/j.jconrel.2005.07.013.

[13] G. Neurauter, S. Scholl-Bürgi, A. Haara, S. Geisler, P. Mayersbach, H. Schennach, D. Fuchs, Simultaneous measurement of phenylalanine and tyrosine by high performance liquid chromatography (HPLC) with fluorescence detection, Clin. Biochem. 46 (2013) 1848–1851, https://doi.org/10.1016/j.clinbiochem.2013.10.015.

[14] M. Alonso, E. Barcia, M. Córdoba-Díaz, S. Negro, D. Córdoba-Díaz, A. Fernández-Carballido, Development and validation of an HPLC method for the quantification of morin flavonoid encapsulated within PLGA nanoparticles, Curr. Pharmaceut. Anal. 17 (2021) 1178–1187, https://doi.org/10.2174/1573412916999200905095914.

[15] P. Marcianes, S. Negro, L. Garcia-Garcia, C. Montejo, E. Barcia, A. Fernandez-Carballido, Surface-modified gatifloxacin nanoparticles with potential for treating central nervous system tuberculosis, Int. J. Nanomed. 12 (2017) 1959–1968, https://doi.org/10.2147/IJN.S130908.

[16] Z. Xu, D.S. Pilch, A.R. Srinivasan, W.K. Olson, N.E. Geacintov, K.J. Breslauer, Modulation of nucleic acid structure by ligand binding: induction of a DNA.RNA. DNA hybrid triplex by DAPI intercalation, Bioorg. Med. Chem. 5 (1997) 1137–1147, https://doi.org/10.1016/s0968-0896(97)00050-3.

[17] M. Vera, E. Barcia, S. Negro, P. Marcianes, L. García-García, K. Slowing, A. Fernandez-Carballido, New celecoxib multiparticulate systems to improve glioblastoma treatment, Int. J. Pharm. 473 (2014) 518–527, https://doi.org/10.1016/j.ijpharm.2014.07.028.

[18] M.D. Abramoff, P.J. Magalhaes, S.J. Ram, Image processing with ImageJ, Biophot. Int. 11 (2004) 36–42.

[19] M.J. Mitchell, M.M. Billingsley, R.M. Haley, M.E. Wechsler, N.A. Peppas, R. Langer, Engineering precision nanoparticles for drug delivery, Nat. Rev. Drug Discov. 20 (2021) 101–124, https://doi.org/10.1038/s41573-020-0090-8.

[20] S. Pragallapati, R. Manyam, Glucose transporter 1 in health and disease, J. Oral Maxillofac. Pathol. 23 (2019) 443–449, https://doi.org/10.4103/jomfp.JOMFP_22_18.

[21] E. Puris, M. Gynther, S. Auriola, K.M. Huttunen, L-Type amino acid transporter 1 as a target for drug delivery, Pharm. Res. 37 (2020) 88, https://doi.org/10.1007/s11095-020-02826-8.

[22] E. Puris, M. Gynther, J. Huttunen, A. Petsalo, K.M. Huttunen, L-type amino acid transporter 1 utilizing prodrugs: how to achieve effective brain delivery and low systemic exposure of drugs, J. Contr. Release 261 (2017) 93–104, https://doi.org/10.1016/j.jconrel.2017.06.023.

[23] K. Bahrami, J. Järvinen, T. Laitinen, M. Reinisalo, P. Honkakoski, A. Poso, K. M. Huttunen, J. Rautio, Structural features affecting the interactions and transportability of LAT1-targeted phenylalanine drug conjugates, Mol. Pharm. 20 (2022) 206–218, https://doi.org/10.1021/acs.molpharmaceut.2c00594.2022.

[24] S. Chen, C. Jin, R. Ohgaki, R, M. Xu, H. Okanishi, Y. Kanai, Structure–activity characteristics of phenylalanine analogs selectively transported by L-type amino acid transporter 1 (LAT1), Sci. Rep. 14 (2024) 4651, https://doi.org/10.1038/s41598-024-55252-w.

[25] R.J. Boado, J.Y. Li, M. Nagaya, C. Zhang, W.M. Pardridge, Selective expression of the large neutral amino acid transporter at the blood-brain barrier, Proc. Natl. Acad. Sci. U.S.A. 96 (1999) 12079–12084, https://doi.org/10.1073/pnas.96.21.12079.

[26] N. Singh, G.F. Ecker, Insights into the structure, function, and ligand discovery of the large neutral amino acid transporter 1, LAT1, Int. J. Mol. Sci. 19 (2018) 1278, https://doi.org/10.3390/ijms19051278.

[27] R. Kannan, R. Chakrabarti, D. Tang, K.J. Kim, N. Kaplowitz, GSH transport in human cerebrovascular endothelial cells and human astrocytes: evidence for luminal localization of Na+-dependent GSH transport in HCEC, Brain Res. 852 (2000) 374–382, https://doi.org/10.1016/s0006-8993(99)02184-8.

[28] Y. Wang, B. Qin, G. Xia, S.H. Choi, FDA's Poly (lactic-co-glycolic acid) research program and regulatory outcomes, AAPS J. 23 (2021) 92, https://doi.org/10.1208/s12248-021-00611-y.

[29] T. Latronico, F. Rizzi, A. Panniello, V. Laquintana, I. Arduino, N. Denora, E. Fanizza, S. Milella, C.M. Mastroianni, M. Striccoli, M.L. Curri, G.M. Liuzzi, N. Depalo, Luminescent PLGA nanoparticles for delivery of darunavir to the brain and inhibition of matrix metalloproteinase-9, a relevant therapeutic target of HIV-associated neurological disorders, ACS Chem. Neurosci. 12 (2021) 4286–4301, https://doi.org/10.1021/acschemneuro.1c00436.

[30] A. Joseph, G.M. Simo, T. Gao, N. Alhindi, N. Xu, D.J. Graham, L.J. Gamble, E. Nance, Surfactants influence polymer nanoparticle fate within the brain, Biomaterials 277 (2021) 121086, https://doi.org/10.1016/j.biomaterials.2021.121086.

[31] F. Madani, H. Morovvati, T.J. Webster, A. Najaf, S. Asaadi, S.M. Rezayat, M. Hadjighassem, M. Khosravani, M. Adabi, Combination chemotherapy via poloxamer 188 surface-modified PLGA nanoparticles that traverse the blood–brain–barrier in a glioblastoma model, Sci. Rep. 14 (2024) 19516, https://doi.org/10.1038/s41598-024-69888-1.

[32] M. Alonso, E. Barcia, J.F. González, C. Montejo, L. García-García, M.C. Villa-Hermosilla, S. Negro, A.I. Fraguas-Sánchez, A. Fernández-Carballido, Functionalization of morin-loaded PLGA nanoparticles with phenylalanine dipeptide targeting the brain, Pharmaceutics 14 (2022) 2348, https://doi.org/10.3390/pharmaceutics14112348.

[33] X. Dong, Current strategies for brain drug delivery, Theranostics 8 (2018) 1481–1493, https://doi.org/10.7150/thno.21254.

[34] H. Hassan, R.O. Bello, S.K. Adam, E. Alias, M.M.R. Meor Mohd Affandi, A. F. Shamsuddin, R. Bassir, Acyclovir-loaded solid lipid nanoparticles: optimization, characterization and evaluation of its pharmacokinetic profile, Nanomaterials 10 (2020) 1785, https://doi.org/10.3390/nano10091785.

[35] E. Joseph, G. Singhvi, Multifunctional nanocrystals for cancer therapy: a potential nanocarrier, in: A.M. Grumezescu (Ed.), Nanomaterials for Drug Delivery and Therapy, first ed., Elsevier Inc., Amsterdam, The Netherlands, 2019, pp. 91–116.

[36] M.D. Cayero-Otero, M.J. Gomes, C. Martins, J. Álvarez-Fuentes, M. Fernández-Arévalo, B. Sarmento, L. Martín-Banderas, *In vivo* biodistribution of venlafaxine-PLGA nanoparticles for brain delivery: plain vs. functionalized nanoparticles, Expet Opin. Drug Deliv. 16 (2019) 1413–1427, https://doi.org/10.1080/17425247.2019.1690452.

[37] K.B. Johnsen, M. Bak, P.J. Kempen, F. Melander, A. Burkhart, M.S. Thomsen, M. S. Nielsen, T. Moos, T.L. Andresen, Antibody affinity and valency impact brain uptake of transferrin receptor-targeted gold nanoparticles, Theranostics 8 (2018) 3416–3436, https://doi.org/10.7150/thno.25228.

[38] C.J. Camacho, Y. Katsumata, D.P. Ascherman, Structural and thermodynamic approach to peptide immunogenicity, PLoS Comput. Biol. 4 (2008) e1000231, https://doi.org/10.1371/journal.pcbi.1000231.

[39] R.J. Boado, J.Y. Li, M. Nagaya, C. Zhang, W.M. Pardridge, Selective expression of the large neutral amino acid transporter at the blood-brain barrier, Proc. Natl. Acad. Sci. U.S.A. 96 (1999) 12079–12084, https://doi.org/10.1073/pnas.96.21.12079.

[40] K. Aoyama, S.W. Suh, A.M. Hamby, J. Liu, W.Y. Chan, Y. Chen, R.A. Swanson, Neuronal glutathione deficiency and age-dependent neurodegeneration in the EAAC1 deficient mouse, Nat. Neurosci. 9 (2006) 119–126, https://doi.org/10.1038/nn1609.

[41] Q. Cai, L. Wang, G. Deng, J. Liu, Q. Chen, Z. Chen, Systemic delivery to central nervous system by engineered PLGA nanoparticles, Am. J. Transl. Res. 8 (2016) 749–764. PMID: 27158367.

[42] W. Geldenhuys, D. Wehrung, A. Groshev, A. Hirani, V. Sutariya, Brain-targeted delivery of doxorubicin using glutathione-coated nanoparticles for brain cancers, Pharmaceut. Dev. Technol. 20 (2015) 497–506, https://doi.org/10.3109/10837450.2014.892130.

[43] P.E. Gilbert, A.M. Brushfield, The role of the CA3 hippocampal subregion in spatial memory: a process oriented behavioral assessment, Prog. Neuro-Psychopharmacol. Biol. Psychiatry 33 (2009) 774–781, https://doi.org/10.1016/j.pnpbp.2009.03.037.

[44] M. Koehl, D.N. Abrous, A new chapter in the field of memory: adult hippocampal neurogenesis, Eur. J. Neurosci. 33 (2011) 1101–1114, https://doi.org/10.1111/j.1460-9568.2011.07609.x.